EXPERIMENTAL STUDIES

Detection of Experimental Right Ventricular Infarction by Isopotential Body Surface Mapping During Sinus Rhythm and During Ectopic Ventricular Pacing

DAVID M. MIRVIS, MD, FACC

Memphis, Tennessee

Electrocardiographic (ECG) effects of experimental, isolated right ventricular infarction were studied in 10 dogs during sinus rhythm as well as during ectopic right and left ventricular pacing. Infarction was produced by injecting latex into the right coronary artery and ECG consequences were examined by body surface isopotential mapping methods using an 84 electrode torso array. During sinus rhythm, subtraction of preinfarction from postinfarction maps demonstrated that right ventricular necrosis produced abnormal negative potentials over the right hemithorax during the early, middle and late portions of the QRS complex. These patterns corresponded to loss of R waves and deepening of preexistent or development of new Q and S waves in waveforms from this region. Patterns during ectopic ventricular stimulation were compared with mean maps derived from 13 control dogs. Both left and right ventricular pacing after right ventricular infarction resulted in a right-sided abnormal minimum, similar in location to that observed during sinus rhythm, throughout the QRS complex.

Thus, 1) right ventricular necrosis does produce QRS complex changes over the right torso that are analogous to those produced by left ventricular infarction, and 2) the dominant pattern of an abnormal right-sided minimum was present regardless of the ventricular activation pattern. This latter finding suggests that the region of right ventricular necrosis provided a supplementary path for current to reenter the heart regardless of the current source, so that an overlying electrode would record negative voltage with all activation patterns.

(J Am Coll Cardiol 1987;10:157–63)

Right ventricular necrosis is a common accompaniment of left ventricular infarction that produces characteristic hemodynamic consequences (1–4). Electrocardiographic (ECG) detection of this clinically important lesion is, however, less completely understood than for damage to the left ventricle. Two possible reasons for this include 1) the limited contribution of the right ventricle to the QRS complex during sinus rhythm because of the simultaneous activation of the dominating left ventricle (5,6), and 2) the masking of the effects of right ventricular damage by the almost universally accompanying left ventricular infarction (1,3).

In this study, we sought to define the ECG abnormalities produced in an experimental model designed to reduce the effects of these two confounding factors. First, infarction was limited to the right ventricle. Second, ECG changes were evaluated using isopotential body surface mapping, a technique known to be sensitive to regional and multiple simultaneously active myocardial wave fronts including those in the right ventricle (7). In addition, we examined the added value of ectopic ventricular pacing to reveal evidence of right ventricular necrosis by permitting sequential rather than simultaneous depolarization of the two ventricles (8,9).

Methods

Experimental model. Right ventricular infarction was experimentally produced in 14 healthy adult dogs (Group A). Anesthesia was induced with intravenous thiopental and maintained by inhalation of an oxygen-halothane-nitrous oxide mixture. We performed a right thoracotomy under sterile conditions, opened the pericardium and isolated the proximal right coronary artery. This vessel was ligated and an arteriotomy was performed distal to the ligature. Liquid latex (1 ml) was then injected into the distal artery to occlude the vessel as well as to "embolize" the collateral vessels

From the Medical Service, Veterans Administration Medical Center and the Department of Medicine, The University of Tennessee, Memphis, Memphis, Tennessee. This study was supported by Grant HL20597 from the National Heart, Lung, and Blood Institute, National Institutes of Health, Bethesda, Maryland and from the Veterans Administration, Washington, D.C.

Manuscript received August 18, 1986; revised manuscript received October 21, 1986, accepted November 17, 1986.

Address for reprints: David M. Mirvis, MD, The University of Tennessee, Memphis, 956 Court Avenue, Room F208, Memphis, Tennessee 38163.

0735-1097/87/$3.50

JACC Vol. 10, No. 1
July 1987:157–63

to it from the other coronary beds (10). Quadripolar epicardial plaque electrodes were sutured onto the right ventricular outflow tract beyond the area of infarction and onto the left ventricular free wall. The chest was closed in layers, and the pacing wires were buried in a subcutaneous pouch near the back of the dog's neck.

An additional 13 dogs served as a control group (Group B). In these, we performed a thoracotomy and implanted pacing electrodes but right coronary artery occlusion was not performed.

ECG recordings. Electrocardiographic signals were recorded before and 3 weeks after surgery. After sedation with Innovar-Vet, 1 to 2 ml intramuscularly, 84 chloridized silver electrodes were placed on the dog's shaved chest. These covered the anterior (54 electrodes) and posterior torso from the level of the clavicles to below the inferior rib margin. Additional electrodes were placed on the legs to record limb leads and to calculate Wilson central terminal voltages.

Potentials from each electrode were amplified and simultaneously digitized at a rate of 500 samples/channel per second. Thoracic electrode voltages were registered using differential amplifiers referenced to the central terminal output.

In the postoperative recording session, signals were sampled during sinus rhythm as well as during ectopic left and right ventricular pacing. The latter was performed using stimuli 2 ms in duration and 50% above diastolic threshold at the lowest rate that permitted reliable capture.

Pathologic studies. Dogs were killed after the second recording session. Hearts were excised and sliced into sections 8 mm thick parallel to the atrioventricular (AV) groove. Sections were then incubated in triphenyltetrazolium chloride solution at 37°C for 30 minutes to delineate infarcted tissue (11). Normal tissue was stained red, whereas necrotic zones remained unstained.

ECG data analysis. ECG potentials were processed to construct isopotential maps, as previously described (12). First, similar QRST cycles were averaged to reduce random noise. Second, onsets and offsets of the QRS and ST-T interval were manually determined from plots of three relatively orthogonal leads. Potentials during a 20 ms period of the terminal TP segment were averaged for use as a zero potential baseline. Isopotential maps were then constructed at 2 ms intervals during the QRS complex using a linear-bilinear interpolation routine.

Isopotential difference maps were constructed to display the changes produced by right ventricular infarction. To do so, potentials at each electrode recorded before surgery were subtracted from those registered at the same locus and at the same instant during the QRS complex after infarction.

Maps displaying the mean potentials at each electrode location during ectopic ventricular pacing were also constructed. To do so, voltages at each site and at each instant during the QRS complex in the 13 control dogs of Group B were averaged. These mean voltages were then processed to form isopotential distributions.

Statistics. Quantitative data were tabulated as mean ± SD. Comparisons using *t* tests relied on a 5% significance level.

Results

Twelve of the 14 Group A dogs subjected to right coronary artery embolization survived the experimental period. At postmortem examination, 10 had extensive necrosis of the right ventricular free wall but without infarction in either the left ventricle or the interventricular septum (Fig. 1). Data from only these 10 dogs were further analyzed.

Sinus rhythm (Fig. 2 to 4). QRS durations changed by 2.4 ± 1.6 ms after infarction ($p > 0.05$). Isopotential maps of Figure 2 demonstrate pre- and postinfarction patterns from one representative case. In each map, plus and minus signs indicate electrode locations, with the sign corresponding to the polarity of the recorded voltage. The center of each map is along the sternum, and the left and right margins correspond to right and left paravertebral regions, respectively. Contour lines, connecting sites at equal potential relative to the Wilson central terminal, are drawn at the levels indicated in each panel. Zero isopotential lines are overdrawn for emphasis, and intensities of the maximal and minimal potentials are tabulated. Electrode sites with peak positive and negative voltages are marked.

Panels A, B and C of Figure 2 depict the potential distribution 14, 32 and 46 ms into the QRS complex before

Figure 1. Heart slice stained with triphenyltetrazolium chloride after latex embolization of the right coronary artery. The unstained region of necrosis **(arrow)** is limited to the right ventricular (RV) free wall. LV = left ventricle.

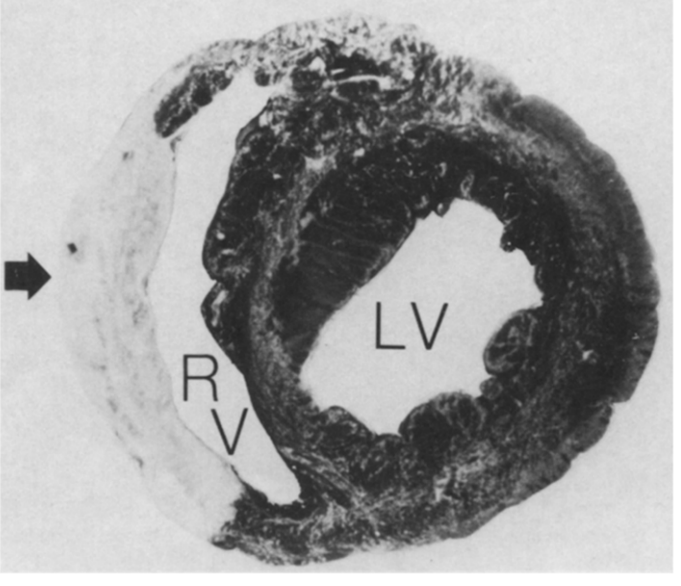

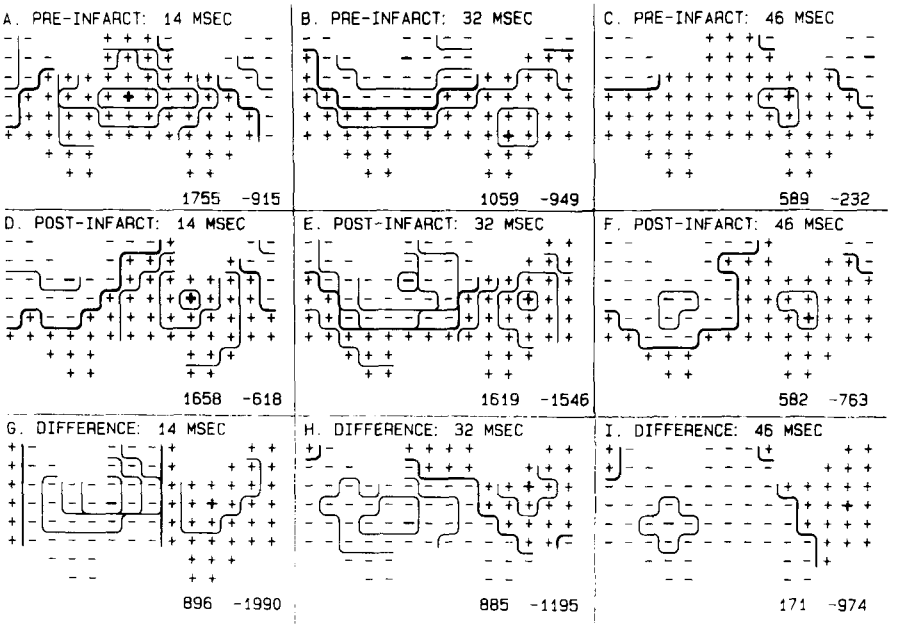

Figure 2. Body surface isopotential maps before (**panels A** to **C**) and after (**panels D** to **F**) right ventricular infarction. **Panels A** and **D,** 14 ms into the QRS complex. **Contour lines** are at zero and ±250 and ±500 μV. **Panels B** and **E,** 32 ms into the QRS complex. **Contour lines** are at zero and ±1,000, ±2,000 and ±2,500 μV. **Panels C** and **F,** 46 ms into the QRS complex. **Contours** are at zero and ±250 and ±500 μV. Maps in **panels G, H** and **I** are isopotential difference maps computed by subtraction of maps in **panels A** to **C** from those in **panels D** to **F.** Markings are as detailed in the text.

infarction. Initially (panel A), a central anterior maximum surrounded superiorly by negative voltages dominates. Subsequently (panel B), negative voltages invaginate into this maximum, resulting in a left lateral maximum and a right superior minimum. Near the end of the QRS complex (panel C), the maximum again moves to a left-central position.

After right ventricular infarction, potentials at each instant were significantly different. Early in the QRS complex (panel D), negative potentials are more prominent as the maximum is shifted laterally. In the midportion (panel E), negative voltages are likewise more prominent over the right hemithorax; terminally (panel F), the right-sided minimum persists. Thus, right ventricular infarction resulted in easily perceived differences in thoracic potentials during all segments of the QRS complex.

Isopotential difference maps highlighted these changes. The map in panel G was constructed by subtraction of the pattern in panel A (14 ms into the QRS complex, preinfarction) from those in panel D (14 ms into the QRS complex, postinfarction). The resulting distribution depicting the electrical field "generated" by infarction was dominated

Figure 3. Examples of the effect of right ventricular infarction on unipolar ECGs registered from six (**A** through **F**) torso electrodes. Positions of the six electrodes are indicated in the diagram on the upper left. Two waveforms from each are illustrated; the left one was recorded before and the right one was registered after right ventricular necrosis. The **scale figure (lower right)** indicates 1 mV vertically and 200 ms horizontally.

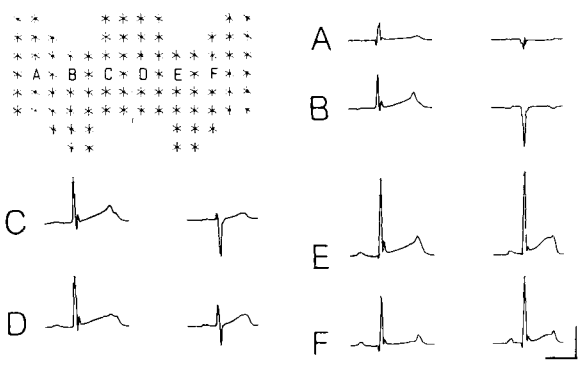

Figure 4. Isopotential distributions 14 ms into the QRS complex before **(panel A)** and after **(panel B)** right ventricular infarction. The **map in panel C** is the result of subtraction of the isopotential distributions in **panel A** from those in **panel B. Contour lines** are drawn at zero and ±500, ±1,000, ±1,500 and ±2,000 μV levels.

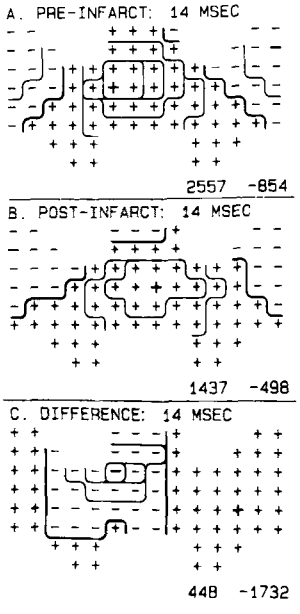

JACC Vol. 10, No. 1
July 1987:157–63

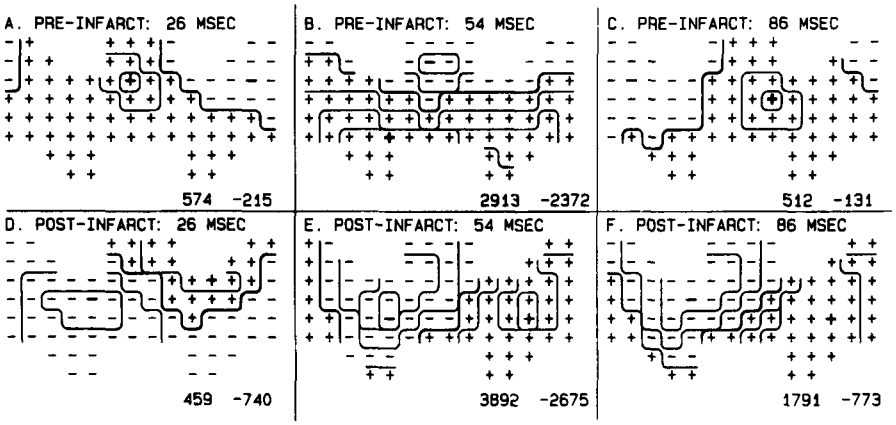

Figure 5. Panels A to **C,** Mean isopotential maps during right ventricular pacing and 26, 54 and 86 ms into the QRS complex. **Panels D** to **F,** Maps from one case after right ventricular infarction during right ventricular pacing at the same instants. **Contour lines** in **panels A, C, D** and **F** are at zero and ±250 and ±500 μV; in **panels B** and **D,** they are at zero and ±1,000, ±2,000 and ±2,500 μV.

by an intense right-sided minimum and a left-sided maximum. During subsequent instants (panels H and I), this right minimum persisted. Thus, right ventricular infarction generated a potential field throughout the QRS complex characterized by a relatively stationary right thoracic minimum and left-sided maximum.

Changes in unipolar ECGs that correspond to the isopotential difference maps are illustrated in Figure 3. Waveforms from right and central thoracic sites (sites A through D) show new Q waves and reduced R wave amplitude after infarction. Those from left torso regions (sites E and F) have increased R wave amplitude. These changes correspond to the location of electrodes in relation to the maxima and minima in difference maps such as in Figure 2 (panels G to I).

Another example is shown in Figure 4. Distributions 14 ms into the QRS complex before (panel A) and after (panel B) infarction are shown. In this case, the overall features of the maps are not different; a central maximum surrounded by superior negativity is observed. The isopotential difference map (panel C), constructed by subtraction of voltages of panel A from those of panel B, reveals an intense right-sided minimum and left-sided maximum. This pattern is like that in Figure 2, panels G to I, and demonstrates the consistency of the effect of right ventricular infarction regardless of the surface ECG pattern.

Right ventricular pacing (Fig. 5). Isopotential distributions during right ventricular pacing without and with right ventricular infarction are shown in Figure 5. Noninfarction patterns in panels A through C represent distributions from average maps computed by determining the mean potential at each electrode site at each instant during the QRS complex in the 13 control dogs of Group B.

In the absence of infarction, early QRS patterns were dominated by a right-sided maximum and a left lateral minimum (panel A). Toward the middle of the QRS complex, the maximum spreads along the caudal torso as the minimum became superiorly and centrally positioned (panel B). Late in the QRS complex, the maximum became left-sided, as negative potentials appeared over the right lateral chest (panel C). The patterns in mean maps were observed in all 13 individual cases.

Patterns from one representative case after right ventricular infarction are shown in panels D through F. Map extrema at 24, 54 and 86 ms into the QRS complex are all similar to each other, but clearly different from those observed at the same time points without infarction (panels A to C). In each map, an intense right-sided minimum exists

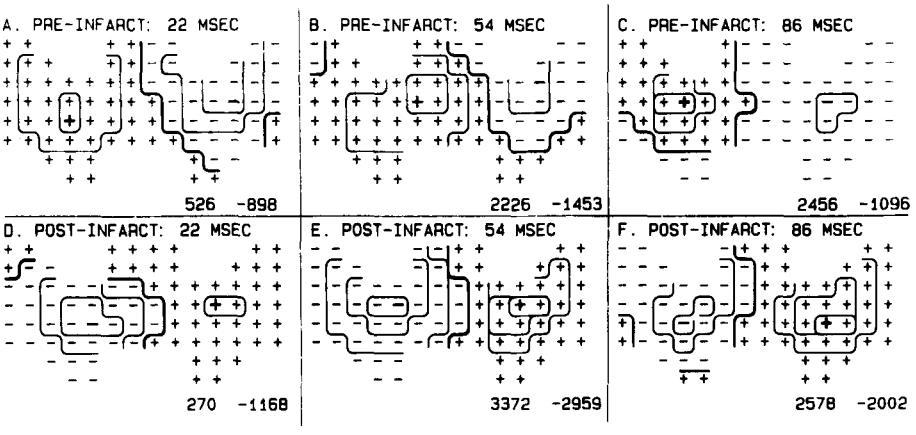

Figure 6. Panels A to **C,** Mean isopotential maps during left ventricular pacing 22, 54 and 86 ms into the QRS. **Panels D** to **F,** Maps from one case after infarction during left ventricular pacing. **Contour lines** as in Figure 5.

that changes in amplitude but not in position. Positive potentials dominate the left hemithorax. These characteristics were seen in all 10 dogs of Group A during right ventricular pacing.

Left ventricular pacing (Fig. 6). Mean maps during left ventricular pacing were constructed from control dogs of Group B as was done for right ventricular stimulation. Patterns are shown in Figure 6, panels A through C. Early during the QRS complex (panel A), a right-sided maximum and a left-sided minimum are observed. This general pattern persists during the mid (panel B) and late QRS (panel C) complex, although changes in low level negative potentials are observed. Such stable patterns were observed in all individual cases as well as in the illustrated mean maps.

After right ventricular infarction, maps at the same time points from one representative case demonstrated a right-sided minimum and a left-sided maximum (panels D to F). Thus, during the early, middle and late QRS complex, isopotential patterns were alike but different from those observed during left ventricular pacing without infarction (panels A to C).

Discussion

Efforts to identify ECG markers of right ventricular infarction may have two motives. First, a noninvasive and accurate method to detect clinically significant lesions would have obvious clinical value. Second, determining the ECG effects of loss of right ventricular tissue may have implications for the pathogenesis of the postinfarction ECG.

Methodology. Results of this study should be considered in relation to the methods used and to prior related efforts. We produced right ventricular infarction by embolization of the right coronary artery. As used in prior studies of left ventricular infarction (10), this produces a dense, homogeneous lesion by blocking retrograde collateral as well as anterograde coronary flow. Similar methods using mercury injections have been reported (4,13,14), as have data documenting the potential significance of collateral flow to the right ventricle (15,16). As illustrated in Figure 1, only cases in which the dense necrosis was limited to the right ventricle were studied, eliminating the confounding factors of patchy necrosis and of left ventricular or septal involvement.

Isopotential mapping was employed because of its proved ability to detect multiple simultaneously active cardiac wave fronts (17,18). This is particularly important when assessing right ventricular phenomena because of the increased likelihood of cancellation of right ventricular forces by the more intense left ventricular forces. For example, evidence of normal right ventricular epicardial breakthrough may be observed simultaneously with potentials generated by continuing left free wall depolarization (7).

Prior studies. Most prior studies have focused on ST segment shifts in right precordial leads (19–26). These efforts generally demonstrated the significant value of ST elevation in various right precordial leads, particularly when recorded soon after the onset of symptoms, in detecting right ventricular infarction. Others have sought QRS abnormalities (14,27–32). Although Myers et al. (27) could not identify changes characteristic of clinical right ventricular involvement, Montague et al. (28) reported differences in Q zone forces in isointegral maps from patients with left ventricular and with biventricular infarction. Experimental studies have similarly described the QRS effects of right ventricular necrosis. Chou et al. (14), for example, reported development of new Q waves and reduction in R wave amplitude over the right side of the chest, that is, the same pattern typical of left ventricular infarction in left-sided leads, after mercury injection into the right coronary artery. These findings corresponded to the minimum in postinfarction isopotential maps published by Sugiyama et al. (29).

Changes during sinus rhythm. Isopotential distributions presented in Figure 2 clearly demonstrate that extensive right ventricular damage does alter the QRS complex. Right-sided negative potentials, most easily seen in the difference maps of panels G to I, are projected to the body surface throughout the period of ventricular depolarization. These findings are similar to those reported by Sugiyama et al. (29), and would correspond to development of Q waves and reduced R wave amplitude in scalar ECG recordings over the right chest (Fig. 3). Thus, right ventricular infarction produces changes analogous to those of left ventricular infarction. The topographic relation of this new postinfarction minimum to the underlying damaged right ventricle is consonant with the documented ability of surface mapping to detect and to localize regional myocardial events, including ischemia and necrosis (18,33).

The value of difference or subtraction maps is emphasized by the data presented in Figure 4. In this case, spatial changes in the directly recorded potential distributions before (panel A) and after (panel B) infarction were small. However, the difference map in panel C demonstrated an intense minimum due to infarction that was very similar to that observed in the example shown in Figure 2 (panel G) that did have more definite postinfarction map changes (panels A and F). Thus, comparison of pre- and postintervention data, a situation that is unfortunately uncommonly possible in the clinic, can identify diagnostically useful data not otherwise detectable.

Changes during ventricular ectopic stimulation. Postinfarction maps during right or left ventricular pacing demonstrated abnormal negative potentials over the right chest throughout the QRS complex when compared with mean, noninfarction distributions (Fig. 5 and 6). Comparison with mean data rather than with individual preinfarction patterns, as was done during sinus rhythm, was required because two operative procedures would have been needed for 1) implantation of electrodes, and 2) production of infarction by embolization.

The most dramatic finding in these studies was the production by right ventricular infarction of a new and abnormal right chest minimum that was spatially stable throughout the QRS complex and that developed regardless of the activation pattern of the ventricles. As shown in Figures 2, 5 and 6, the postinfarction distributions were similar during sinus rhythm, right ventricular pacing and left ventricular stimulation, all of which produce very different activation sequences and surface patterns in the absence of infarction.

This uniform response was unexpected. Wilson et al. (33) proposed that an infarction produces an electrically inert or passive "hole" through which an electrode views activity on the opposite heart surface. If so, alteration of activation patterns should likewise alter the potentials registered by an electrode overlying the infarct in periods of the QRS complex during which the infarcted region was normally active. Such changes in excitation may result from either the normal temporal sequence of activation or global changes produced by bundle branch block or ectopic stimulation. No such effects were observed despite the large size and homogeneity of the experimentally produced right ventricular infarction; both would augment the "window" function of the lesion.

The observed similarities may, however, be interpreted according to an alternative ECG role for the necrotic tissue suggested by Flaherty et al. (34). As illustrated by these investigators, the inactive necrotic zone provides a path of nondepolarized myocardium through which torso currents can reenter the heart chambers. In this view, the negativity over the infarct is the result of active rather than passive factors. Accordingly, an electrode positioned over the reentry site would register negative potentials regardless of the site of origin of the current flows, that is, the activation front. As location of active sites varied, current would flow from their endocardial margins, through the epicardium and around the torso to reenter through the infarct. (Transmural activation is largely in an endocardial to epicardial direction even with epicardial stimulation [9].) Hence, the polarity of voltage recorded over the lesion would be negative regardless of the activation sequence, as was observed here. Variations in low amplitude contours might reflect the differences in source location.

Duration of the negativity would vary with the period of inactivity of the infarcted region. In the case of dense right ventricular infarction, the persistence of negativity throughout the QRS complex is consistent with the dense transmural lesion producing complete electrical silence.

Left versus right ventricular infarction. Although mid and late QRS changes do occur with left ventricular infarction, they are typically positive rather than negative voltage shifts (35), possibly related to effects of local conduction block. This difference between right and left ventricular infarction may relate to the heterogeneous lesions in the left ventricle with epicardial and scattered intramural sparing produced by coronary ligation rather than to the dense, transmural right ventricular necrosis produced by latex injection. Spared tissue may be activated late in the QRS complex (36), rendering the infarct zone active rather than inactive, producing local positive voltages. It may be speculated that lesions produced in the left ventricle by these two methods would also differ in their electrocardiologic properties.

References

1. Wackers FJ Th, Lie KI, Sokole EB, Res J, van der Schoot J, Durrer D. Prevalence of right ventricular involvement in inferior wall infarction assessed with myocardial imaging with thallium-201 and technetium-99m pyrophosphate. Am J Cardiol 1978;42:358–62.
2. Isner JM, Roberts WC. Right ventricular infarction complicating left ventricular infarction secondary to coronary heart disease. Am J Cardiol 1978;42:885–94.
3. Ratliff NB, Hackel DB. Combined right and left ventricular infarction: pathogenesis and clinicopathologic correlations. Am J Cardiol 1980;45: 217–21.
4. Goldstein JA, Vlahakes GJ, Verrier ED, et al. The role of right ventricular systolic dysfunction and elevated intrapericardial pressure in the genesis of low output in experimental right ventricular infarction. Circulation 1982;65:513–22.
5. Durrer D, van Dam R Th, Freud GE, Janse MJ, Meijler FL, Arzbaecher RC. Total excitation of the isolated human heart. Circulation 1970;41:899–912.
6. Spach MS, Barr RC. Ventricular intramural and epicardial potential distributions during ventricular activation and repolarization in the intact dog. Circ Res 1975;37:243–57.
7. Taccardi B. Distribution of heart potentials on dog's thoracic surface. Circ Res 1962;11:862–9.
8. Walston A, Boineau JP, Spach MS, Ayers CR, Estes EH. Relationship between ventricular depolarization and QRS in right and left bundle branch block. J Electrocardiol 1968;1:155–60.
9. Spach MS, Barr RC. Analysis of ventricular activation and repolarization from intramural and epicardial potential distributions for ectopic beats in the intact dog. Circ Res 1975;37:830–43.
10. Euler DE, Prood CE, Moore EN. The interruption of collateral blood flow to the ischemic canine myocardium by embolization of a coronary artery with latex: effects on conduction delay and ventricular arrhythmias. Circ Res 1981;49:97–108.
11. Fishbein MC, Meerbaum S, Rit J, et al. Early phase acute myocardial infarct size quantification: validation of the triphenyl tetrazolium chloride tissue enzyme staining technique. Am Heart J 1981;101:593–600.
12. Mirvis DM, Gordey RL. Electrocardiographic effects of myocardial ischemia induced by right atrial pacing in dogs with coronary stenosis. I. Repolarization changes with progressive left circumflex coronary arterial narrowing. J Am Coll Cardiol 1983;1:1090–8.
13. Lluch S, Moguilevsky HC, Pietra G, Shaffer AB, Hirsch LJ, Fishman AP. A reproducible model of cardiogenic shock in the dog. Circulation 1969;39:205–18.
14. Chou T-C, Fowler NO, Gabel M, van der Bel-Kahn J, Feltner EJ. Electrocardiographic and hemodynamic changes in experimental right ventricular infarction. Circulation 1983;67:1258–67.
15. Ramo BW, Peter RH, Ratliff N, Kong Y, McIntosh HO, Morris JJ. The natural history of right coronary arterial occlusion in the pig. Am J Cardiol 1970;26:156–61.
16. Peter RH, Ramo BW, Ratliff N, Morris JJ. Collateral vessel development after right ventricular infarction in the pig. Am J Cardiol 1972;29:56–60.
17. Abildskov JA, Burgess MJ, Lux RL, Wyatt RF. Experimental evi-

dence for regional cardiac influence in body surface isopotential maps of dogs. Circ Res 1976;38:386–91.

18. Mirvis DM, Keller FW, Ideker RE, Cox JW, Zettergren DG, Dowdie RF. Values and limitations of surface isopotential mapping techniques in the detection and localization of multiple discrete epicardial events. J Electrocardiol 1977;10:347–58.

19. Erhardt LR, Sjogren A, Wahlberg I. Single right-sided precordial lead in the diagnosis of right ventricular involvement in inferior myocardial infarction. Am Heart J 1976;91:571–6.

20. Candell-Riera J, Figueras J, Valle V, et al. Right ventricular infarction: relationships between ST segment elevation in V_{4R} and hemodynamic, scintigraphic, and echocardiographic findings in patients with acute inferior myocardial infarction. Am Heart J 1981;101:281–7.

21. Chou T-C, van der Bel-Kahn J, Allen J, Brockmeier L, Fowler NO. Electrocardiographic diagnosis of right ventricular infarction. Am J Med 1981;70:1175–80.

22. Croft CH, Nicod P, Corbett JR, et al. Detection of right ventricular infarction by right precordial electrocardiography. Am J Cardiol 1982;50: 421–7.

23. Braat SH, Brugada P, DeZwaan C, Coenegracht JM, Wellens HJJ. Value of electrocardiogram in diagnosing right ventricular involvement in patients with an acute inferior wall myocardial infarction. Br Heart J 1983;49:368–72.

24. Klein HO, Tordjman T, Ninio R, et al. The early recognition of right ventricular infarction: diagnostic accuracy of the electrocardiographic V_4R lead. Circulation 1983;67:558–65.

25. Geft I, Shah PK, Rodriguez L, et al. ST elevation in leads V_1 to V_5 may be caused by right coronary artery occlusion and acute right ventricular infarction. Am J Cardiol 1984;53:991–6.

26. Lopez-Sendon J, Coma-Canella I, Alcasena S, Seoane J, Gamallo C. Electrocardiographic findings in acute right ventricular infarction: sensitivity and specificity of electrocardiographic alterations in right precordial leads V_4R, V_3R, V_1, V_2 and V_3. J Am Coll Cardiol 1985;6: 1273–9.

27. Myers GB, Klein HA, Hiratzka T. Correlation of electrocardiographic and pathologic findings in infarction of the interventricular septum and right ventricle. Am Heart J 1949;37:720–70.

28. Montague TJ, Smith ER, Spencer CA, et al. Body surface electrocardiographic mapping in inferior myocardial infarction. Circulation 1983;67:665–73.

29. Sugiyama S, Wada M, Sugenoya J, Toyoshima H, Toyama J, Yamada K. Diagnosis of right ventricular infarction: experimental study through the use of body surface isopotential maps. Am Heart J 1977;94:445–52.

30. Medrano GA, de Michelli A. Right posterior ventricular necrosis. An experimental study. J Electrocardiol 1979;12:197–204.

31. Warner RA, Hill NE, Spear R, et al. Vectorcardiographic manifestations of experimental right ventricular necrosis. J Electrocardiol 1981;14:175–80.

32. Warner RA, Hill NE, Spear R, Mookherjee S, Smulyan H. Detection of experimental right ventricular necrosis using vectorcardiograms obtained during artificial pacing. J Electrocardiol 1982;15:119–25.

33. Wilson FW, Johnston FD, Hill IGW. The form of the electrocardiogram in experimental myocardial infarction. IV. Additional observations on the later effects produced by ligation of the anterior descending branch of the left coronary artery. Am Heart J 1935;10: 1025–41.

34. Flaherty JT, Spach MS, Boineau JP, Canent RV, Barr RC, Sabistan DC. Cardiac potentials on body surface of infants with anomolous left coronary artery (myocardial infarction). Circulation 1967;36:345–58.

35. Flowers NC, Horan LG, Johnson JC. Anterior infarctional changes occurring during mid and late ventricular activation detectable by surface mapping techniques. Circulation 1976;54:906–13.

36. Boineau JR, Cox JL. Slow ventricular activation in acute myocardial infarction. A source of re-entrant premature ventricular contraction. Circulation 1973;48:702–13.